01 Sep 2002

Morphologic and Magnetic Properties of $Pd_{100-x}Fe_x$ Nanoparticles Prepared by Ultrasound Assisted Electrochemistry

Maribel Guzman

Jean Luc Delplancke

Gary J. Long
Missouri University of Science and Technology, glong@mst.edu

Jacques P. Delwiche

et. al. For a complete list of authors, see https://scholarsmine.mst.edu/chem_facwork/824

Recommended Citation

M. Guzman et al., "Morphologic and Magnetic Properties of $Pd_{100-x}Fe_x$ Nanoparticles Prepared by Ultrasound Assisted Electrochemistry," *Journal of Applied Physics*, vol. 92, no. 5, pp. 2634-2640, American Institute of Physics (AIP), Sep 2002.
The definitive version is available at https://doi.org/10.1063/1.1497463

Morphologic and magnetic properties of $Pd_{100-x}Fe_x$ nanoparticles prepared by ultrasound assisted electrochemistry

Maribel Guzman and Jean-Luc Delplancke[a)]
Materials Science and Electrochemistry Laboratory, CP 194/03, Université Libre de Bruxelles, 50 Avenue Roosevelt, B-1050 Brussels, Belgium

Gary J. Long
Department of Chemistry, University of Missouri-Rolla, Rolla, Missouri 65409-0010

Jacques Delwiche
Thermodynamique et Spectroscopie Institute of Chemistry, B6, Université de Liège, B-4000 Sart-Tilman, Belgium

Marie-Jeanne Hubin-Franskin[b)]
Laboratoire de Spectroscopie d'Electrons Diffusés Institute of Chemistry, B6, Université de Liège, B-4000 Sart-Tilman, Belgium

Fernande Grandjean[c)]
Institute of Physics, B5, Université de Liège, B-4000 Sart-Tilman, Belgium

(Received 23 January 2002; accepted for publication 6 June 2002)

Nanopowdered alloys of $Pd_{100-x}Fe_x$, with $x=4$, 6, 8, and 12, have been prepared by ultrasound assisted electrochemistry. The composition of the individual particles, as determined by x-ray fluorescence, and the bulk composition, as determined by atomic absorption, are in agreement within experimental error. Transmission electron microscopy indicates that the nanopowders consist of agglomerates of small grains with a radius of approximately 5 nm, a radius which is confirmed by the broadening of the reflections in the x-ray powder diffraction patterns. X-ray fluorescence analysis of individual grains indicates a homogeneous distribution of palladium and iron throughout the grains. The x-ray diffraction patterns indicate that solid solutions of iron in palladium show no evidence of any pure palladium, any pure iron, or any other PdFe compound. The 78 K iron-57 Mössbauer spectra of these nanopowders reveal the presence of one magnetic sextet assigned to slowly relaxing superparamagnetic particles of $Pd_{100-x}Fe_x$ and one weak doublet, which is assigned to rapidly relaxing superparamagnetic particles of $Pd_{100-x}Fe_x$. The hyperfine fields of 29.0 to 31.0 T are typical of iron in a metallic alloy and correspond to a magnetic moment of approximately 2 μ_B per iron atom. The hysteresis curves obtained at 4.2, 100, and 295 K with a vibrating sample magnetometer are typical of superparamagnetic particles with saturation magnetization values which are substantially smaller than those observed for the bulk. The fit of the magnetization curves with a Langevin function yields estimates of the particle radii which are in good agreement with those obtained both by transmission electron microscopy and by the broadening of the x-ray diffraction peaks. © *2002 American Institute of Physics.* [DOI: 10.1063/1.1497463]

I. INTRODUCTION

The sensitivity of the magnetic properties of palladium to the introduction of $3d$ transition-metal impurities has been a puzzle[1–10] for the past 40 years. Extensive attention has been devoted to the so-called giant magnetic moment[11–13] of iron in the palladium-rich PdFe alloys. Indeed, whereas magnetic susceptibility and magnetization measurements in the palladium-rich PdFe alloys yield iron magnetic moments[1,11,12] varying between 5 and 12.6 μ_B, depending upon the iron content, Mössbauer-effect hyperfine field[6] measured in zero field and neutron diffraction[4] measurements yield iron magnetic moments of approximately 2 and 3 μ_B, respectively. Further, Mössbauer-effect hyperfine field measurements carried out under an applied field between 0.5 and 4 K with ^{57}Co electroplated into Pd show[14,15] Brillouin behavior with a magnetic moment of 12 μ_B. The apparent disagreement between the macroscopic magnetic measurements and the iron microscopic measurements can be understood[13] if a small magnetic moment of approximately 0.05 μ_B is induced on each of the 200 or so palladium atoms surrounding the iron moment via a strong ferromagnetic itinerant electron polarization of the palladium $4d$ electrons.

More recently, magnetic measurements[8,16] on pure palladium particles of less than 6.4 nm radius have revealed ferromagnetic properties with a magnetic moment of 0.23 ± 0.19 μ_B per palladium atom. Further, fine particles of palladium containing 2.9 at. % of iron, particles which were prepared by a gas evaporation technique, show[8] a magnetic behavior which can be understood in terms of a core/shell

a)Author to whom correspondence should be addressed; electronic mail: jdelpla@ulb.ac.be
b)Directeur de Recherches, FNRS, Belgium.
c)Electronic mail: fgrandjean@ulg.ac.be

model. In this model, the outer shell is nonmagnetic and the core shows an enhanced saturation magnetization compared to that of a bulk PdFe alloy. Hence, particle size has a dramatic influence on the magnetic behavior of both pure palladium and palladium-rich PdFe alloys.

Fine and ultrafine metallic particles with diameters between 5 and 100 nm have[17] many applications, for instance, in catalytic chemistry and magnetic recording. Indeed, palladium is a widely used but expensive catalyst whose recovery is economically important. If a pure palladium catalyst could be replaced by a magnetic palladium-rich PdFe alloy catalyst, then the catalyst could be magnetically removed from the reaction products. Unfortunately, there are[18] very few cost-effective nanopowder production methods. Some of us have recently developed[19,20] an ultrasound-assisted electropulse technique for the production of transition-metal magnetic nanopowders. The cost of this technique is especially low, the composition of the powder is easily controlled, and the homogeneity of the grains is excellent. Hence, it is of value to prepare, by ultrasound-assisted electrochemistry, nanopowders of palladium-rich PdFe alloys, and to study their morphologic and magnetic properties. Thus, we report herein the preparation and chemical analysis of nanopowders of $Pd_{100-x}Fe_x$ alloys, with x equal to 4, 6, 8, and 12. These nanopowders have been structurally and morphologically characterized by x-ray diffraction and transmission electron microscopy. Further, we report the macroscopic and microscopic magnetic properties of these nanopowders as determined by vibrating sample magnetometry and iron-57 Mössbauer spectroscopy.

II. EXPERIMENT

A recently designed and locally constructed electropulse apparatus which has been described in detail earlier[20] has been used for the preparation of the PdFe nanopowders. The high-intensity ultrasound is generated by a titanium piezoelectric horn operated at its fundamental resonance frequency of 20 kHz with a power of approximately 50 W/cm^2, i.e., just above the cavitation threshold of the electrolyte solution. At intensities above this cavitation threshold, a cloud of bubbles is produced[20] below the tip of the horn. A pulsed ultrasound mode is used in which the pulse duration is 100 ms. The start of each ultrasound pulse is triggered by the potentiostat. The titanium horn is controlled by a Tacussel PRT 20-10X potentiostat which is used to adjust the current density passing through the tip of the horn. Dissolved oxygen is removed from the electrolyte by degassing for one hour with pure argon before each preparation. The potentiostat is operated in the pulsed mode with an on time of 100 ms and a duty cycle, $t_{on}/(t_{on}+t_{off})$ of 0.33, where t_{on} and t_{off} are the time on and time off of the electrochemical pulse, respectively.

The electrolyte composition is 0.45 mol/l of $FeSO_4 \cdot 7H_2O$, 2.1×10^{-4} mol/l of $PdCl_2$, 0.48 mol/l of H_3BO_3, and 0.017 mol/l of citric acid. The electrolyte pH is 3.8 and the bath temperature is maintained at 333 K. The cell uses a palladium anode and a mercury sulfate reference electrode. The current density J, used for each alloy is given in Table I.

TABLE I. Composition of individual crystallites and the bulk powder of the $Pd_{100-x}Fe_x$ alloys.

		Energy dispersive x-ray analysis[a]		Atomic absorption[a]	
Alloy	J (A/m^2)	Pd	Fe	Pd	Fe
$Pd_{96}Fe_4$	2500	96	4	97	3
$Pd_{94}Fe_6$	3500	94	6	95	5
$Pd_{92}Fe_8$	4500	92	8	94	6
$Pd_{88}Fe_{12}$	5500	88	12	83	17

[a]The values are given in atomic percent and the estimated errors are ±1 at. %.

After three hours of deposition, the suspensions are filtered under argon with a 0.1 μm Millipore filter or a 0.01 μm Whatman filter. The powders are washed with pure ethanol, filtered, and dried at room temperature under argon.

III. NANOPOWDER COMPOSITION AND MORPHOLOGY

The compositions and homogeneity of the individual $Pd_{100-x}Fe_x$ alloy particles have been determined by x-ray fluorescence with a Philips EDAX apparatus connected to a Philips CM 20 scanning transmission electron microscope. The bulk compositions of the powders have also been measured with a Perkin-Elmer 2380 atomic absorption instrument. The compositions obtained by these two techniques agree within experimental error except for the highest-iron content sample, see Table I. In this article, we will designate the different samples by the compositions obtained from the electron diffraction x-ray analysis.

The x-ray diffraction patterns of the nanopowders have been obtained with a Siemens D5000 diffractometer with copper K_α radiation. The patterns obtained for the nanopowders are shown in Fig. 1. In this figure, the bars indicate the reflections expected for pure palladium and the observed peaks for the nanopowders have been assigned to these known reflections. However, as expected, the observed peaks

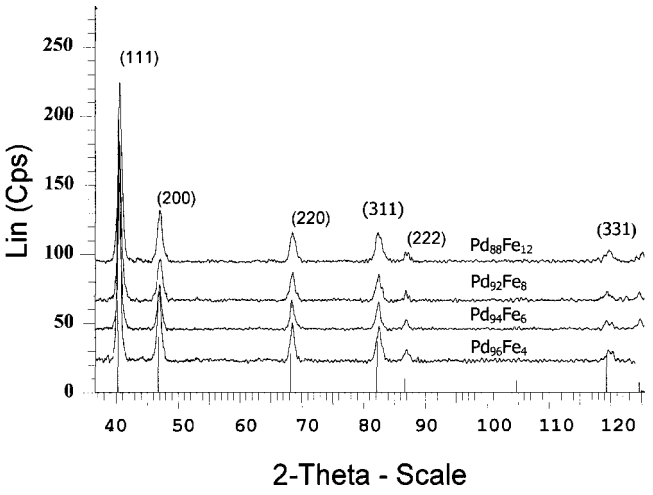

FIG. 1. X-ray diffraction patterns of the indicated nanopowders. The bars indicate the diffraction peaks for pure palladium.

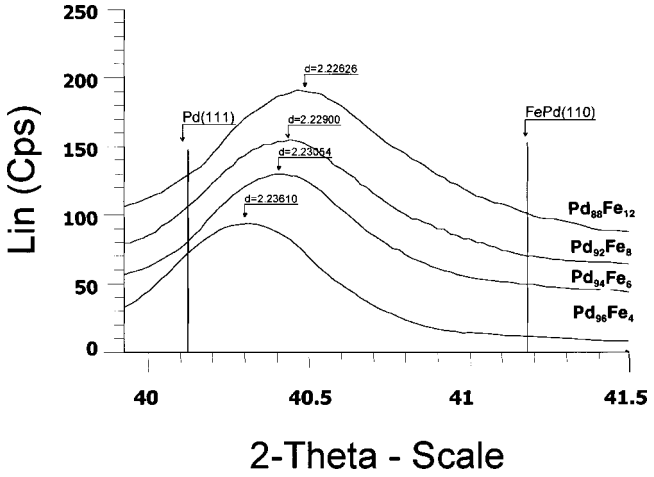

FIG. 2. The (111) reflection for the indicated nanopowders. The bars indicate the (111) reflection for palladium and the (110) reflection for the stoichiometric compound PdFe.

are shifted to higher 2θ angles with increasing iron content. This shift is better observed in Fig. 2 in which the (111) reflections of the four nanopowders are shown along with the known reflection positions of both pure palladium and PdFe which is a stoichiometric compound. In conclusion, the x-ray diffraction patterns indicate both that all the nanopowders are solid solutions of iron in palladium, with a unit-cell volume that decreases with increasing iron content, and that they contain no stoichiometric impurities, such as PdFe or $PdFe_3$. Further, within the detection limit of approximately 3 at. % no iron oxides are observed.

The high-energy electron diffraction rings observed for $Pd_{96}Fe_4$ are shown in Fig. 3. The rings observed for the remaining three nanopowders are similar to those shown in Fig. 3 and all the results are characteristic of the fcc palladium crystal structure with slightly reduced lattice parameters. The electron diffraction results are in complete agreement with the x-ray diffraction results.

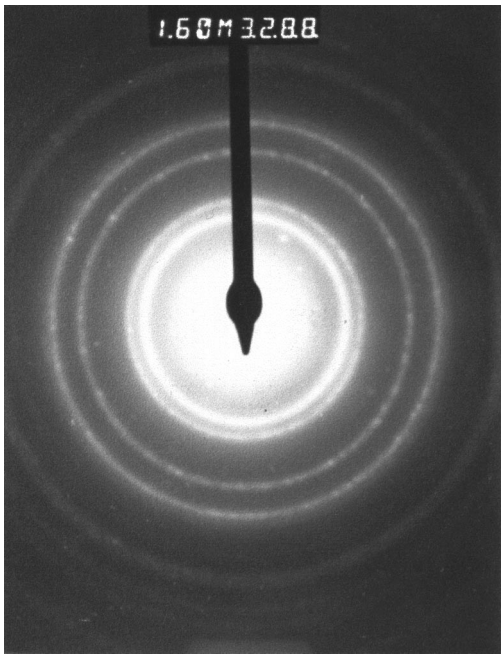

FIG. 3. Electron diffraction rings for $Pd_{96}Fe_4$.

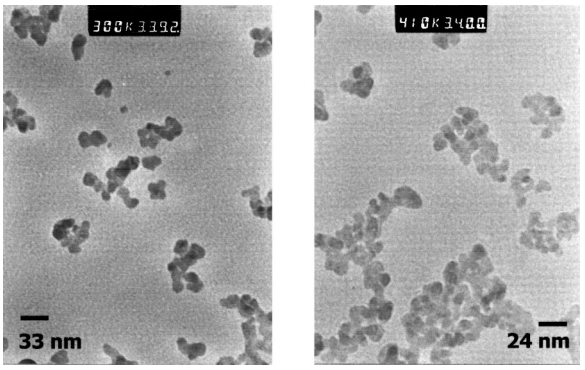

FIG. 4. Transmission electron microscopy photographs of $Pd_{94}Fe_6$ (left) and $Pd_{88}Fe_{12}$ (right).

The transmission electron microscopy photographs for $Pd_{94}Fe_6$ and $Pd_{88}Fe_{12}$, shown in Fig. 4, indicate that the nanopowders consist of well-dispersed agglomerates of grains with a narrow size distribution. The size of the agglomerates is between 50 and 100 nm, whereas the radius of the individual particles is approximately 5 nm. The radius of the particles, as determined from the broadening of the reflections in the x-ray powder diffraction patterns, is given in Table II and decreases from 14 ± 3 nm for $Pd_{96}Fe_4$ to 8 ± 2 nm for $Pd_{88}Fe_{12}$. Such small particles are expected[21] to consist of single magnetic domains.

A mapping of the elemental composition of individual nanoparticle clusters has been performed by x-ray fluorescence analysis. The results indicate the presence of only palladium and iron. A nanoparticle cluster of $Pd_{88}Fe_{12}$ and its mapping with both the iron K_α and palladium L_α emission lines are shown in Fig. 5. This figure clearly reveals that iron and palladium are uniformly distributed throughout the cluster, a cluster that is thus completely homogeneous. The remaining three alloys exhibit similar excellent homogeneities.

IV. MAGNETIZATION MEASUREMENTS

The magnetization measurements were obtained with an Oxford Instruments MagLab VIT-9 vibrating sample magnetometer. The magnetization curves were measured at differ-

TABLE II. Size and magnetic properties of the $Pd_{100-x}Fe_x$ alloy nanopowders.

	$Pd_{96}Fe_4$	$Pd_{94}Fe_6$	$Pd_{92}Fe_8$	$Pd_{88}Fe_{12}$
r^a (nm)	14(3)	12(2)	10(2)	8(2)
r^b (nm)	11(1)	9(1)	7(1)	6(2)
M_s^c (Am^2/kg)	2.75	3.72	6.00	8.30
H_c^d (T)	0.01	0.01	0.01	0.01
T_c^e (K)	122	162	220	240

[a]Radii determined from the broadening of the x-ray diffraction peaks.
[b]Radii obtained from the fit of the magnetization curves as described in the text.
[c]Saturation magnetizations at 4.2 K.
[d]Coercive fields at 4.2 K.
[e]Curie temperatures of the bulk alloys as reported in Ref. 1.

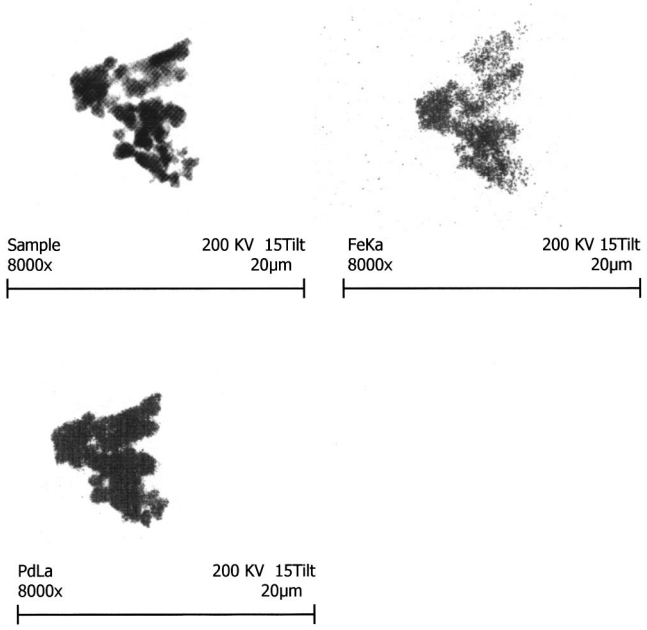

FIG. 5. The x-ray fluorescence mapping of $Pd_{88}Fe_{12}$ for the total emission, and the iron K_α and the palladium L_α emission lines.

ent temperatures by scanning the superconducting coil at a 0.2 T/min rate. The magnetometer was calibrated with nickel with a magnetization of 55.18 Am^2/kg at 295 K in a field of 0.6 T. The measurements were corrected for the contribution of the sample holder. The samples were first zero-field cooled to 4.2 K, then a field of 2 T was applied to center the sample in the pickup coils of the magnetometer, finally, the field was swept from 0 to 8 T, then through 0 to −8 T, and finally, through 0 to 8 T.

The magnetization curves at 4.2, 100, and 295 K for $Pd_{92}Fe_8$ are shown in Fig. 6. The three remaining samples exhibit a similar behavior. At 4.2 K, the magnetization saturates in an applied field of 0.5 T, but, in contrast, at 100 and 295 K, it does not saturate even at 8 T. Such behavior is often

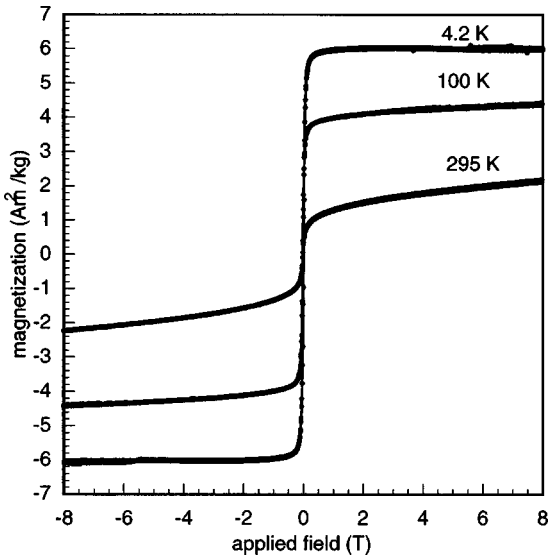

FIG. 6. The magnetization curves obtained at 4.2, 100, and 295 K for $Pd_{92}Fe_8$.

observed[22] for small particles exhibiting superparamagnetism. Superparamagnetic behavior is not unexpected for PdFe particles with a radius of approximately 5 nm, the value observed by transmission electron microscopy. Indeed, the estimated[21] single-domain particle size for equiatomic PdFe is about 35 nm.

The magnetization curves shown in Fig. 6 have been fit[22] with the function

$$M(H) = L(V\rho M_s H/kT) + aH, \tag{1}$$

where

$$L(V\rho M_s H/kT) = M_s[\coth(V\rho M_s H/kT) - kT/V\rho M_s H] \tag{2}$$

and $L(V\rho M_s H/kT)$ is the Langevin function, V is the average volume of the particle, ρ is the density of the particle, M_s is the saturation magnetization, k is the Boltzmann constant, T is the temperature, H is the applied field, and a is a coefficient corresponding to the slope of the magnetization at higher-applied fields. The density of palladium, 12×10^3 kg/m^3, was used in these fits. At 4.2 K, a is zero and the field dependence of the magnetization could be fit with only the Langevin function. At 100 and 295 K, it was necessary to include the second term in Eq. (1) in order to account for the observed slope in the magnetization between 2 and 8 T. The fit is satisfactory at 100 K, but the poorer fit obtained at 295 K indicates that the approximation[22] of the Langevin function (2) is not fully adequate. This inadequacy is likely to result from a narrow distribution of particle sizes and from a small distribution in the composition. From Eq. (1), an estimate of the average particle volume V may be obtained and the corresponding radii for a spherical particle is given in Table II. These values are in excellent agreement with the radius measured in the transmission electron micrographs and determined from the broadening of the x-ray diffraction peaks. At 4.2 K, anomalously small volumes are obtained apparently because, at 4.2 K, the small particles are interacting collectively[22] and behave like a soft ferromagnet with a small coercive field. The small coercive fields observed in the $Pd_{100-x}Fe_x$ alloys are given in Table II.

The 4.2 K saturation magnetizations for $Pd_{96}Fe_4$, $Pd_{94}Fe_6$, $Pd_{92}Fe_8$, and $Pd_{88}Fe_{12}$ are given in Table II. The measured saturation magnetizations are all substantially smaller than the 77 K saturation magnetizations,[1] ranging from 13 to 45 Am^2/kg, for bulk PdFe alloys with similar compositions. Because, as shown by the x-ray fluorescence mapping of the grains, see Sec. III, the composition of the grains is very homogeneous, this drastic decrease in saturation magnetization can only be ascribed to the small size of the particles. The 4.2 K saturation magnetizations, obtained at 8 T for both $Pd_{96}Fe_4$ and $Pd_{97.1}Fe_{2.9}$ fine particles[8] are plotted as a function of the particle radius in Fig. 7, along with the extrapolated[1] value for the $Pd_{96}Fe_4$ bulk alloy. This figure clearly indicates that the saturation magnetizations are strongly dependent upon the radius of the particle and that the bulk value is not reached for particle radii of less than 40 nm. A similar size dependence[21] of the magnetization of ultrafine FePd particles has already been observed and was ascribed to both surface oxidation and the palladium-rich

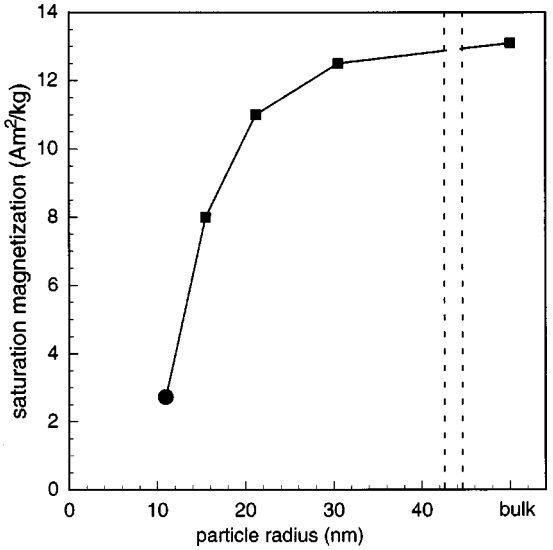

FIG. 7. The dependence of the saturation magnetization upon particle size for $Pd_{96}Fe_4$, solid circle, and the $Pd_{97.1}Fe_{2.9}$ alloys, solid squares, from Ref. 8.

core of the particles. The size dependence of the magnetization observed in Fig. 7 cannot be ascribed to surface oxidation of the particles which are rich in palladium and do not show any oxide phase in their x-ray diffraction patterns. We believe that in the nanoparticles the polarization of the $4d$ palladium electrons by the iron magnetic moment is not very effective. In the case of palladium clusters, Vitos, Johansson, and Kollar[23] have suggested a different size effect on the magnetic properties, i.e., a change in structure from the usual fcc structure to an icosahedral structure for particles with a radius of approximately 3.4 nm. However, the x-ray diffraction patterns shown in Figs. 1 and 2 do not suggest any structural changes in the nanopowders studied herein.

We believe that the linear term in Eq. (1) represents a fraction of the sample that at both 100 and 295 K is above its curie temperature and is thus paramagnetic. The Curie temperatures[1] of the bulk palladium-rich PdFe alloys are given in Table II. It is well known[22] that the Curie temperature of nanoparticles of composition similar to the bulk is usually smaller than the Curie temperature of the bulk. Hence, at 100 and 295 K, it is expected that a fraction of the nanopowders behaves like a paramagnet.

V. MÖSSBAUER SPECTRAL RESULTS

The Mössbauer spectra for the nanopowders, obtained at 78 K, are shown in Fig. 8. The Mössbauer spectra were obtained on a constant-acceleration spectrometer which utilized a room-temperature rhodium matrix cobalt-57 source and was calibrated at room temperature with α-iron foil. The absorber thicknesses ranged from 60 to 80 mg/cm^2.

Because both only a small amount of material was available and because the iron content is very low in $Pd_{96}Fe_4$ and $Pd_{94}Fe_6$, the signal-to-noise ratio of the Mössbauer spectra of these absorbers is rather low but is sufficient to give results which can be compared with those obtained for the samples with a larger amount of iron.

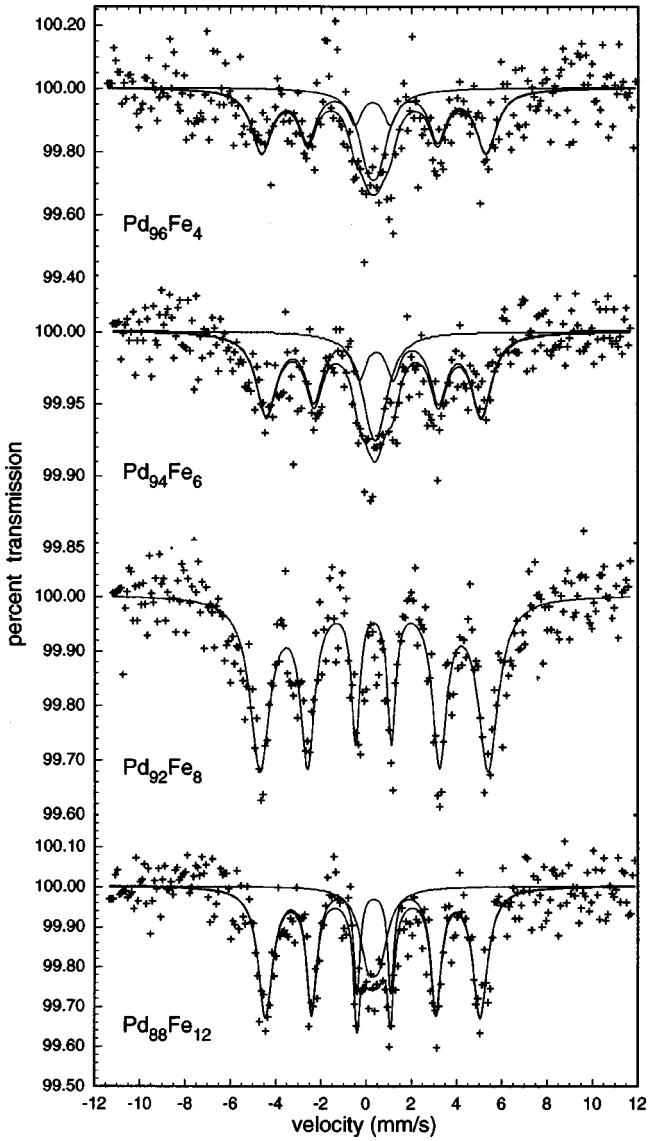

FIG. 8. Mössbauer spectra of the $Pd_{100-x}Fe_x$ alloy nanopowders obtained at 78 K.

The spectra have been fit with a broadened magnetic sextet and a doublet which has an isomer shift that is the same as the sextet. The magnetic sextet is characteristic of palladium-rich $Pd_{100-x}Fe_x$ alloy fine particles below their blocking temperature, and the doublet probably results from iron in small superparamagnetic particles above their blocking temperature. The spectral parameters resulting from this analysis are given in Table III. The estimated errors are ± 0.02 mm/s for the isomer shift δ, the quadrupole splitting ΔE_Q, and the linewidth Γ, ± 0.5 T for the hyperfine fields H, and $\pm 2\%$ for the percent area, except for $Pd_{96}Fe_4$, for which the estimated errors are ± 0.1 mm/s, ± 1 T, and $\pm 5\%$ respectively. The isomer shift of the magnetic sextet is independent of the iron content and agrees well with the earlier value[24] of 0.3 mm/s. The hyperfine fields also agree well with earlier values.[3,6] Further, as is shown in Fig. 9, the hyperfine field shows some indication of an oscillatory behavior with iron content. This oscillatory behavior is, at least to some extent, in agreement with the calculated[25] dependence on iron con-

TABLE III. Mössbauer spectral parameters of the $Pd_{100-x}Fe_x$ nanopowders obtained at 78 K.

Alloy	δ[a] (mm/s)	H (T)	ΔE_0 (mm/s)	Γ (mm/s)	Area (%)
$Pd_{96}Fe_4$	0.31	30.7	0.06[b]	0.72	70
	0.31	-	0.47	1.07	30
$Pd_{94}Fe_6$	0.40	29.4	−0.10[b]	0.72	72
	0.40	-	0.31	1.15	28
$Pd_{92}Fe_8$	0.34	31.2	0.02[b]	0.43	100
$Pd_{88}Fe_{12}$	0.32	29.4	−0.04[b]	0.32	79
	0.32	-	0.50	0.91	21

[a]Relative to room temperature α-iron foil.
[b]The quadrupole shift for the magnetically ordered spectral components.

tent of the hyperfine field in the $Pd_{100-x}Fe_x$ alloys, a dependence which is plotted as the solid line in Fig. 9. But unfortunately the quality of the data prevents any firm confirmation of the calculation. From the hyperfine field of approximately 30.0 T, an iron magnetic moment of approximately 2.0 μ_B can be deduced. Hence, we can conclude on the basis of their hyperfine parameters, that the microscopic properties of the iron in the fine particles of $Pd_{100-x}Fe_x$ alloys do not differ from those in the bulk alloys.

VI. DISCUSSION AND CONCLUSIONS

Magnetic nanopowders of $Pd_{100-x}Fe_x$ alloys, with $x \leqslant 12$, have been prepared by ultrasound-assisted electrochemical deposition. Electron microscopy studies indicate that the powders consist of agglomerates, with a size of between 50 and 100 nm, of grains with a radius of between 5 and 10 nm. The composition of the powder is well controlled by the composition of the electrolytical bath and the x-ray fluorescence mapping of the grains shows a very homogeneous distribution of palladium and iron in the grains. The x-ray diffraction analysis confirms that the $Pd_{100-x}Fe_x$ alloys crystallize in the fcc structure of palladium with a unit-cell volume decreasing with increasing iron content.

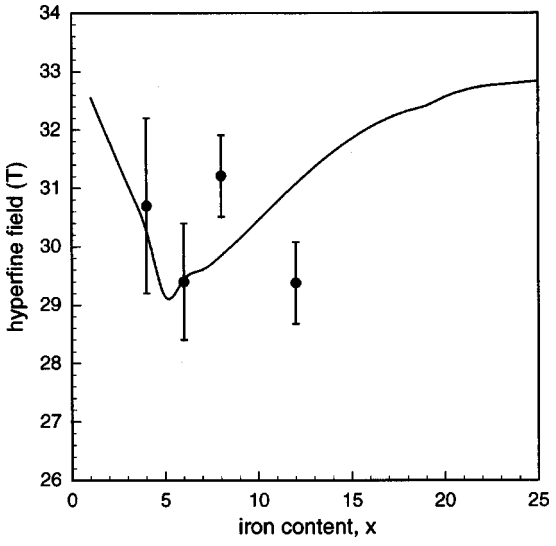

FIG. 9. The compositional dependence of the hyperfine field in the $Pd_{100-x}Fe_x$ nanopowders. The solid line is the calculated hyperfine field from Ref. 25.

Within the time domain of the magnetization measurements, i.e., about 10 s or more, the prepared powders consist of superparamagnetic particles with an average radius of approximately 6 to 11 nm, at 100 and 295 K, particles which at 4.2 K, reach a collective state similar to that of a soft ferromagnet probably as a result of strong dipolar interactions between the magnetic moments of the individual particles. Within the time domain of Mössbauer spectroscopy, approximately 10^{-8} s, at 78 K, the $Pd_{100-x}Fe_x$ alloy powders consist of a mixture of both small particles, which undergo slow relaxation of their magnetic moments and thus exhibit static hyperfine fields, and even smaller particles, which undergo rapid relaxation of their magnetic moments and thus exhibit quadrupole doublets. The two different techniques, magnetization and Mössbauer spectroscopy, have very different time domains and give somewhat differing pictures of the $Pd_{100-x}Fe_x$ alloys.

The 4.2 K saturation magnetization values of the nanopowders are much smaller than the giant magnetizations observed for bulk $Pd_{100-x}Fe_x$ alloys with the same or similar iron contents. Hence, we conclude that the polarization of the $4d$ band of palladium by the iron $3d$ electrons is much less effective in particles of approximately 5 nm radius than in larger particles. From the observed saturation magnetization of 2.75 Am^2/kg for $Pd_{96}Fe_4$, we can calculate a moment of 0.05 μ_B per alloy atom, a value which is reasonable and substantially smaller than the value of 0.23 ± 0.19 μ_B observed[8] in small particles of pure palladium. If we assume that the moments result only from the iron, we obtain a moment of approximately 1.6 μ_B per iron, a value which is in good agreement with the 2.0 μ_B value obtained from the Mössbauer spectral hyperfine fields. Alternatively, a paramagnetic shell-ferromagnetic core model[16] of the particles may account for the reduced saturation magnetizations observed in particles with radii of a few nanometers.

In conclusion, the size dependence of the macroscopic and microscopic magnetic properties of nanopowders, particularly of $Pd_{100-x}Fe_x$ nanopowder alloys, must be further investigated both theoretically and experimentally. We plan the preparation and study of iron-57-enriched nanopowders of $Pd_{100-x}Fe_x$ alloys with x values up to 50. Calculations of the magnetic properties of small clusters or grains of $Pd_{100-x}Fe_x$ nanopowder alloys with x of 1 to 5 are also required to further understand the relationship between a particles size and its magnetic properties.

ACKNOWLEDGMENTS

The authors thank Mr. A. Mohan for his help in obtaining the Mössbauer spectra. The authors acknowledge with thanks the financial support of the US National Science Foundation through Grant No. DMR-95-21739 and the Fonds National de la Recherche Scientifique, Belgium, through Grant No. 9.456595, the Fonds de la Recherche Fondamentale Collective, Belgium, through Grant Nos. 2.4531.00F and 2.4522.01, the University of Liège through budget Grant No. 2850006. Marie-Jeanne Hubin-Franskin

acknowledges support from the Fonds National de la Recherche Scientifique, Belgium, as a Directeur de Recherches. M. Guzman thanks the Coopération Universitaire au Développement du Conseil Interuniversitaire de la Communauté Française de Belgique, for Grant No. D35097.

[1] J. Crangle, Philos. Mag. **5**, 335 (1960).
[2] P. P. Craig, D. E. Nagle, W. A. Steyert, and R. D. Taylor, Phys. Rev. Lett. **9**, 12 (1962).
[3] D. E. Nagle, P. P. Craig, P. Barrett, D. R. F. Cochran, C. E. Olsen, and R. D. Taylor, Phys. Rev. **125**, 490 (1962).
[4] J. W. Cable, E. O. Wollan, and W. C. Koehler, J. Appl. Phys. **34**, 118 (1963).
[5] P. P. Craig, R. C. Perisho, R. Segnan, and W. A. Steyert, Phys. Rev. **138**, A146 (1965).
[6] P. E. Clark and R. E. Meads, J. Phys. C **3**, S30 (1970).
[7] R. A. Levy, J. J. Burton, D. I. Paul, and J. I. Budnick, Phys. Rev. B **9**, 1085 (1974).
[8] T. Taniyama, E. Ohta, T. Sato, and M. Takeda, Phys. Rev. B **55**, 977 (1997).
[9] Y. Tsunoda and R. Abe, Phys. Rev. B **55**, 11 507 (1997).
[10] R. M. Bozorth, P. A. Wolff, D. D. Davis, V. B. Compton, and J. H. Wernick, Phys. Rev. **122**, 1157 (1961).
[11] A. M. Clogston, B. T. Mathias, M. Peter, H. J. Williams, E. Corenzwit, and R. J. Sherwood, Phys. Rev. **125**, 541 (1962).
[12] G. J. Nieuwenhuys, Adv. Phys. **24**, 515 (1975).
[13] J. A. Mydosh and G. J. Nieuwenhuys, in *Ferromagnetic Materials*, Vol. 1, edited by E. P. Wohlfarth (North-Holland, Amsterdam, 1980).
[14] T. A. Kitchens, W. A. Steyert, and R. D. Taylor, Phys. Rev. **138**, A467 (1965).
[15] M. P. Maley and R. D. Taylor, J. Appl. Phys. **38**, 1249 (1967).
[16] T. Taniyama, T. Sato, E. Ohta, and M. Takeda, Physica B **213–214**, 254 (1995); T. Taniyama, E. Ohta, and T. Sato, Europhys. Lett. **38**, 195 (1997); T. Taniyama, E. Ohta, and T. Sato, Physica B **237–238**, 286 (1997).
[17] *Nanophase Materials: Synthesis-Properties-Applications*, edited by G. C. Hadjipanayis and R. W. Siegel (Kluwer Academic Publishers, Dordrecht, 1994).
[18] I. Malsch, *Nanotechnology in Europe: Experts' Perceptions and Scientific Relations Between Sub-areas*; European Commission-JRC Institute for Prospective Technological Studies, EUR 17710 EN, ECSC-EEC-EAEC: Brussels, 1997.
[19] R. Winand, J. Reisse, and J.-L. Delplancke, Belgian Patent 1994, No. 09400555, Dispositif pour la production de poudres ultrafines.
[20] J.-L. Delplancke, J. Dille, J. Reisse, G. J. Long, A. Mohan, and F. Grandjean, Chem. Mater. **12**, 946 (2000).
[21] L. Yiping, G. C. Hadjipanayis, C. M. Sorensen, and K. J. Klabunde, J. Appl. Phys. **75**, 5885 (1994).
[22] J. L. Dormann, D. Fiorani, and E. Tronc, in *Advances in Chemical Physics*, Vol. XCVIII, edited by I. Prigogine and S. A. Rice (Wiley, New York, 1997).
[23] L. Vitos, B. Johansson, and J. Kollar, Phys. Rev. B **62**, R11 957 (2000).
[24] G. Bemski, Phys. Lett. **18**, 213 (1965).
[25] F. M. Galperin and F. G. Kizhaev, Phys. Status Solidi B **66**, 389 (1974).